JOURNAL OF VIROLOGY, May 2000, p. 4214–4219 Vol. 74, No. 9
0022-538X/00/$04.00+0
Copyright © 2000, American Society for Microbiology. All Rights Reserved.

Frequent Homologous Recombination Events between Molecules of One RNA Component in a Multipartite RNA Virus

A. BRUYERE, M. WANTROBA, S. FLASINSKI,† A. DZIANOTT, AND J. J. BUJARSKI*

Plant Molecular Biology Center and Department of Biological Sciences, Northern Illinois University, DeKalb, Illinois 60115, and Institute of Bioorganic Chemistry, Polish Academy of Sciences, Poznan, Poland

Received 18 October 1999/Accepted 2 February 2000

Brome mosaic bromovirus (BMV), a tripartite plus-sense RNA virus, has been used as a model system to study homologous RNA recombination among molecules of the same RNA component. Pairs of BMV RNA3 variants carrying marker mutations at different locations were coinoculated on a local lesion host, and the progeny RNA3 in a large number of lesions was analyzed. The majority of doubly infected lesions accumulated the RNA3 recombinants. The distribution of the recombinant types was relatively even, indicating that both RNA3 counterparts could serve as donor or as acceptor molecules. The frequency of crossovers between one pair of RNA3 variants, which possessed closely located markers, was similar to that of another pair of RNA3 variants with more distant markers, suggesting the existence of an internal recombination hot spot. The majority of crossovers were precise, but some recombinants had minor sequence modifications, possibly marking the sites of imprecise homologous crossovers. Our results suggest discontinuous RNA replication, with the replicase changing among the homologous RNA templates and generating RNA diversity. This approach can be easily extended to other RNA viruses for identification of homologous recombination hot spots.

It is generally accepted that RNA recombination contributes significantly to the diversity of viruses with RNA genomes (37). However, little experimental evidence supports the occurrence of high-frequency recombination in the virus life cycle. The processes of RNA replication and RNA recombination have been studied extensively in brome mosaic bromovirus (BMV), a tripartite positive-strand RNA virus (12). BMV RNA1 and RNA2 code, respectively, for the 1a and 2a proteins (the viral components of the replicase complex), while RNA3 encodes the 3a (movement) and coat proteins (2). Both homologous and nonhomologous recombination events have been observed among different BMV RNAs (24). Homology-supported crossovers can occur between two nearly identical RNAs (or within nearly identical regions), while nonhomologous crosses can occur between nonrelated RNAs or dissimilar regions (8, 16, 29). The frequency of homologous intersegmental crosses in BMV is approximately 10-fold higher than that of the nonhomologous crosses (24). In addition to BMV, homologous RNA recombination has been demonstrated for picornaviruses (18–20, 35), coronaviruses (21, 23, 42), for cowpea chlorotic mottle bromovirus (3), tombusviruses (41), and bacteriophages (31). Homology-driven recombination of non-replicative RNA precursors has been reported for Sindbis virus within the overlapping sequences (34).

Homologous crossovers among different BMV RNA segments appear to require common 15- to 60-nucleotide (nt) sequences (26) which are composed of GC-rich regions followed by AU-rich regions (27, 28). A proposed template-switching mechanism (27, 28) predicts that the replicase enzyme pauses (stalls) at the AU-rich sequence on a donor BMV RNA molecule and switches to the acceptor template while the upstream GC-rich region facilitates the hybridization of the nascent RNA (27, 28).

There is little information about homologous recombination among a population of viral RNA molecules during virus replication, because most of the recombinants may not differ from the parental RNA. The crossovers in poliovirus RNAs were observed at various locations within the 190-nt region between two selectable marker mutations (20, 35). No striking sequence specificity of crossover sites was found, but the crossovers tended to occur within the potential inter- and intramolecular double-stranded (heteroduplex) regions (1). Homologous crossovers were also observed among genomic RNAs of strains of the coronavirus mouse hepatitis virus (22, 40, 42). The RNA crosses have occurred at apparent hot spots (6), but later data revealed that some of the hot spots resulted from selection of mouse hepatitis virus variants (5).

To investigate the contribution of homologous recombination in the RNA virus life cycle, we have studied in vivo the crossovers between molecules of BMV RNA3. Pairs of RNA3, carrying marker mutations at distant locations, were used to measure the frequency of recombination in *Chenopodium quinoa*, a BMV local-lesion host. The homologous RNA3-RNA3 recombinants accumulated at high frequency in local lesions that were doubly infected with different combinations of the RNA3 variants. The frequency of crossovers between one pair of RNA3 variants which possessed the closely located markers was similar to that of another pair of RNA3 variants with more distant markers, suggesting the existence of an internal recombination hot spot. We discuss the implications of these results in terms of the mechanism of RNA recombination, viral RNA genetics, and evolution.

MATERIALS AND METHODS

Materials. Plasmids pB1TP3, pB2TP5, and pB3TP7 (17) were used as templates to synthesize in vitro the infectious capped transcripts of wild-type (wt) BMV RNA1, RNA2, and RNA3, by using the MEGAscript T7 kit (Ambion, Austin, Tex.). Plasmids SF23, SF25, SF29, and SF30 (see the next paragraph) were used to synthesize the RNA3 mutants in the in vitro transcription reactions.

* Corresponding author. Mailing address: Plant Molecular Biology Center, Department of Biological Sciences, Northern Illinois University, DeKalb, IL 60115. Phone: (815) 753-0601. Fax: (815) 753-7855. E-mail: jbujarski@niu.edu.

† Present address: Monsanto, St. Louis, MO 63198.

The Moloney murine leukemia virus reverse transcriptase (RT) and the restriction enzymes were from Promega Corp. (Madison, Wis.).

Generation of RNA3 mutants. The four BMV RNA3 mutants SF23, SF25, SF29, and SF30 were derived from the wt cDNA clone of RNA3, pB3TP7 (17). Each of the four mutated RNA3 components was obtained using different procedures. Mutant SF23 was created by site-directed mutagenesis, during which the nucleotide U-121 was replaced with an A. This mutation created a *Bam*HI restriction site and was translationally silent. For mutant SF25, two nucleotides (AU) were introduced in the 3′ untranslated region (position 1862) in the RNA3 molecule, and this resulted in a new restriction site (*Bam*HI). The RNA3 mutant SF29 (also named BX4) was selected from infected *Chenopodium hybridum* leaves (as described in reference 9). The use of *C. hybridum* plants in BMV recombination was originally reported by Rao et al. (33). SF29 has a 12-nt [$(GAUC)_3$] insertion at position 860, resulting in suppression of the unique *Bcl*I restriction site and addition of 4 amino acids (Pro-Ser-Ile-Asp) between the residues Asp-257 and Gln-258. Mutant SF30 (previously named D1 [13]) was selected as a pseudorevertant from a single local lesion on *C. hybridum* after inoculation with a frameshift mutant D (9). Mutant SF30 contains three additional U residues inserted at two separate locations, resulting in replacement of Trp-22–Thr-23 with Phe-Ser-Gly in the coat protein. Both SF29 and SF30 are derived from SF25 by introducing appropriate mutations into the parental RNA3 variants.

In vivo recombination assays. Equal amounts of pairs of RNA3 mutants were coinoculated with wt RNA1 and wt RNA2 on *C. quinoa* leaves, as previously described (25). A mixture of 1 μg of each transcript in 15 μl of the inoculation buffer solution (10 mM Tris [pH 8.0], 1 mM EDTA, 0.1% Celite) was inoculated onto a fully expanded leaf. In each experiment, four separate leaves per plant (two to three plants) were inoculated. Each inoculation experiment was repeated two or three times. The inoculated *C. quinoa* plants were maintained in a standard greenhouse. Local lesions were counted, collected 14 days postinoculation, and stored at −80°C.

Cloning and analysis of recombinants. For each parental RNA3-RNA3 mutant combination, total RNA was isolated from separate local lesions as described previously (25) and the full-length RNA3 recombinants were amplified as cDNA, using RT-PCR, as described previously (25).

Primer AB75 (5′-CAGTGAATTCTGGTCTCTTTTAGAGATTTACAGTG-3′), which was used for the first-strand cDNA synthesis with MMLV RT, was complementary to nt 2093 to 2117 of the 3′ terminus of RNA3. The resulting 2.2-kb cDNA products were amplified by PCR using *Taq* DNA polymerase and primers AB6 (5′-CGGAATTCGTAAAATACCAACTAATTCTCGTTCG-3′), which annealed to nt 1 to 26 at the 5′ end of wt BMV RNA3, and AB270 (5′-GGGTTCTTCCGAAGAGAG-3′), which was complementary to nt 2026 to 2009. The PCR products were purified with the QIAquick gel extraction kit (Qiagen Inc.) and ligated into the 3′ T overhangs of cloning vector pGEM-T Easy (Promega Corp.). The ligation mixtures were transformed to *Escherichia coli* DH5α and plated on 2× YT agar (tryptone-yeast extract-sodium acetate) containing ampicillin (100 μg/ml), 5-bromo-4-chloro-3-indolyl-β-D-galactopyranoside (X-Gal) (for blue-white selection), and isopropyl-β-D-thiogalactopyranoside (IPTG). Positive clones were screened by PCR using primers AB6 and AB270. The PCR fragments were purified and digested with *Bam*HI and *Bcl*I and analyzed on a 1.5% agarose gel. To partially sequence the purified PCR products, we used primers AB10 (5′-CTGTTGATCAGGTTGCCCAGGAAGA TTTG-3′) and AB4 (5′-GGCCTTGCCTTGGCCAGCAGCGAG-3′), which annealed, respectively, to nt 855 to 882 and nt 1376 to 1353 of BMV RNA3.

Control RT-PCR amplifications. Control experiments were performed to rule out the possibility of recombinant artifacts being generated by the RT-PCR amplifications. The transcribed BMV RNA3 mutants were mixed in pairs (SF23 × SF25, SF23 × SF29, SF23 × SF30, and SF29 × SF30), 100 ng each, and used directly as templates for RT-PCR amplification with primers AB6 and AB270. These PCR fragments were then cloned and analyzed, as described above.

RESULTS

Infectivity and in vivo stability of RNA3 mutants. Figure 1 shows the location of the sequence modifications present in the four parental BMV RNA3 variants SF23, SF25, SF29, and SF30. The infectivity of the SF mutants was determined on *C. quinoa*, a local-lesion host for BMV. The transcribed RNA3s for each mutant were mixed with transcribed RNA1 and RNA2 and inoculated on the leaves. The time necessary for the appearance of the local lesions and the number and size of the local lesions did not differ between the mutants and wt infections (data not shown). However, based on virus purification yield, mutants SF25, SF29, and SF30 accumulated five to six times less than did wt virus, while SF23 accumulated two to three times less than did the wt virus.

As determined by restriction analysis of the RT-PCR products (based on sequencing of 15 clones of each SF variant [data not shown]), the progeny of the four RNA3 mutants from *C. quinoa* contained the originally introduced (or disabled) restriction sites, which confirmed the stability of the RNA3 mutants during infection. It also revealed that the RT-PCR procedure used did not modify the restriction site sequences.

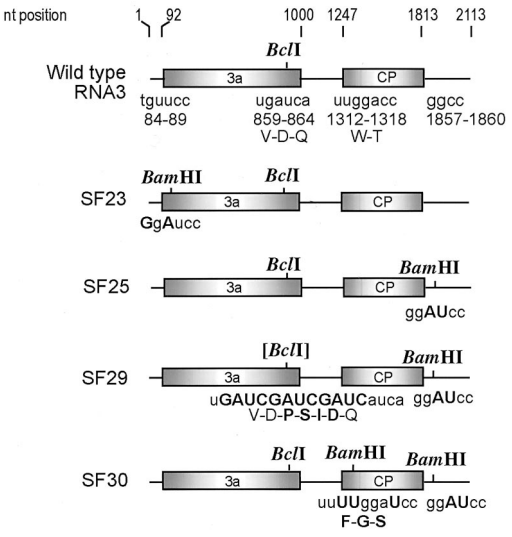

FIG. 1. Location of marker mutations in the BMV RNA3 variants. Lines represent the noncoding regions, while shaded boxes represent open reading frames for 3a and for the coat protein (CP). The modified nucleotides and amino acids are shown below, in bold type. The numbers on top represent nucleotide positions in the wt sequence, marking the beginning and end of each of the noncoding and the coding regions. The disabled *Bcl*I site marker mutation in SF29 is indicated within square brackets (the third line).

Coinfection with mutants SF23 and SF25. In RNA3 variant combination SF23 and SF25, the marker restriction sites (*Bam*HI) were introduced at the 3′ and 5′ ends, providing a 1.73-kb window for recombination (Fig. 1). The coinoculation with variants SF23 and SF25 could theoretically lead to the appearance of two kinds of recombinants, R1 and R2 (Fig. 2),

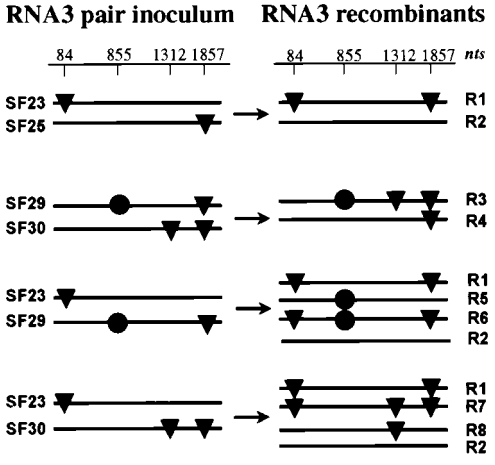

FIG. 2. Location of marker mutations in pairs of BMV RNA3 variants and in the projected homologous recombinants (designated R1 through R8). Solid triangles and circles represent *Bam*HI and disabled *Bcl*I sites, respectively. The numbers on the top scale give the location of marker mutations. The predicted RNA3 recombinants include only those that arose due to a single crossover event between the coinfecting parental RNA3 variants. Recombinants R5, R6, and R8 were not identified in these experiments.

TABLE 1. Restriction analysis of the RT-PCR products from the progeny BMV RNA after infection with pairs of SF RNA3 variants

Mutant RNA3 pair[a] and expt no.	Total no. of local lesions analyzed	Restriction profile[b]				
		SF23	SF25	SF29	SF30	Both parents and/or recombinant(s)
SF23 × SF25						
1	5	3	2			0
2	34	16	3			15
3	31	11	16			4
4	15	3	10			2
SF29 × SF30						
1	5			1	4	0
2	20			0	18	2
3	39			0	33	6
4	14			1	13	0
5	37			0	31	6
SF23 × SF29						
1	19	19		0		0
2	31	31		0		0
SF23 × SF30						
1	18	14			0	4
2	49	47			0	2

[a] Plants were coinoculated with four different combinations of BMV RNA3 variants: SF23 × SF25, SF29 × SF30, SF23 × SF29, and SF23 × SF30 (left column). RT-PCR products were obtained from the RNAs extracted from the local lesions and analyzed as described in Materials and Methods.

[b] The numbers represent the number of local lesions that have accumulated either the parental or the parental and/or the recombinant (the last column) restriction profiles.

TABLE 2. Distribution of the parental and recombinant cDNA clones of the progeny RNA3 variants in the individual doubly infected local lesions[a]

Mutant RNA3 pair and lesion no.	Restriction profile[b]									
	SF23	SF25	R1	R2	SF29	SF30	R3	R4	R7	R8
SF23 × SF25										
1			1							
2			1							
3	1		1							
4			1							
5				2						
6			1							
13	2			1						
18	6		1	1						
19	4	1	3	2						
25	1		1							
28	1	2	2	1						
31	3	1	1	1						
34			1	3						
57	12	2								
60	1	9								
62	1	1	1	2						
118	8		4	1						
SF29 × SF30										
1							1			
5						2		1		
23						7		1		
24						4		1		
30						3	2	2		
61					1	3	3	2		
96					3	7	2	1		
98					13	1		1		
103					1	6		1		
110	4	2	4		4	2	4	1		
SF23 × SF30										
3				1		3			2	
12				3		1			1	
18	1			1		16			1	
29	4			3		6			2	
39	3					4				
50				2		1			1	

[a] The progeny RNA3 was amplified by RT-PCR using total RNA extracts obtained from separate, doubly infected local lesions (Table 1, last column), and the resulting cDNA products were cloned, as described in Materials and Methods. Several clones from each separate lesion were analyzed by digestion with the restriction enzymes.

[b] The number of individual clones representing the particular recombinant (or parental) restriction profiles.

since each of the marker mutants could serve as a donor or as an acceptor molecule. The restriction analysis of the RT-PCR cDNA products from 85 lesions (of four independent experiments) revealed that 75% of the lesions contained a single parental RNA3 variant (Table 1). Within this group of local lesions, the individual parental RNA3 variants were represented evenly, reflecting similarities between SF23 and SF25 in their ability to induce infection.

Twenty-one (nearly 25%) of the local lesions contained both parental RNA3 variants. The PCR products of doubly infected local lesions were cloned and analyzed by digestion with *Bam*HI and *Bcl*I to determine the recombinant profiles. From 2 of 17 lesions analyzed (lesions 57 and 60), only parental SF23 and SF25 clones were obtained (Table 2). Of the remaining 15 lesions, 8 accumulated one type of recombinant (R1 or R2) while 7 accumulated both recombinants. Recombinant R1 appeared in 13 lesions (19 clones), while R2 appeared in 9 lesions (14 clones), suggesting that both molecules can serve as donor or acceptor with an equal chance. These results demonstrate that SF23 and SF25 can coreplicate, can recombine, and can continue to replicate in the presence of R1 or R2.

Twenty of the R1 or R2 clones were sequenced within the intercistronic region (with primers AB10 and AB4) to determine the precision of homologous recombination in this likely region of crossovers. Of the 20 clones, 14 contained the unchanged wt sequence while 6 displayed modifications (data not shown). In particular, out of four clones of local lesion 19, one had a single insertion (an A) at position 1116, one had a single substitution (A to G) at position 995 (changing Ile-302 to Val in the C terminus of protein 3a), one had a silent A-to-G substitution at position 1242, and one had a T-to-C and two A-to-G substitutions, respectively, at positions 1154 (silent), 1275 (Met-9 to Val), and 1333 (Gln-20 to Arg) (both in the coat protein gene). Also, in local lesion 118, one clone had a silent T-to-C exchange at position 925 and one had a double AC-to-TA substitution (silent) at positions 1123 to 1124. These data seem to suggest that in some local lesions the homologous crossovers can lead to sequence modifications (see also reference 26) and that crossovers can occur in RNA3 within both open reading frames and within the intercistronic region. However, another possibility is that these mutations can arise due to simple misinsertion during nonrecombinational copying (see the next paragraph).

Control experiments were performed to determine whether sequence modifications, which have been introduced as marker mutations, could affect the crossover events within the intercistronic region. The cDNA clones were obtained by RT-PCR amplification of the progeny BMV RNA3 from separate SF23

or SF25 infections and were compared with those from wt infection. Twenty clones from each group were sequenced. Similar to the SF23 × SF25 infection, for each individual infection six to eight clones displayed either single-nucleotide substitutions or single-nucleotide insertions (data not shown). The distributions of the observed changes were similar to those for the SF23 × SF25 infection. Again, this sequence variability could be either due to imprecise homologous crossovers or due to the BMV replicase errors. Control RT-PCR experiments for the amplification errors, which are described in a separate section below, show that the *Taq*1 polymerase errors are less likely to contribute to the observed mutations.

Coinfection with mutants SF29 and SF30. Since marker mutations in the combination SF23 × SF25 were far apart from one another, no specific region(s) active in recombination could be mapped on the sequence of RNA3. To reduce the size of the overlapping region, another pair of mutated RNA3 recombinants (SF29 × SF30) was used, where the marker mutations (the lost *Bcl*I and the new *Bam*HI sites) were separated by only 460 nt (Fig. 1). The expected recombinants R3 and R4 are shown in Fig. 2.

The analysis of the progeny RNA3 (cumulative of five independent experiments) of SF29 × SF30 inoculations is shown in Table 1. Similar to the SF23 × SF25 combination, the majority (88%) of the local lesions tested (a total of 115 lesions were analyzed) contained only one parental RNA3 variant, with 2% of them containing SF29 and 98% containing SF30. This shows that SF30 can overcome SF29. However, the recombinant clones appeared in 14 local lesions (12%). Of the 10 lesions analyzed, 5 (i.e., 50%) contained single recombinants (either R3 or R4), 4 accumulated both recombinant types, and 1 did not accumulate recombinants (Table 2). The total number of clones identified as recombinant R3 or R4 was similar (12 and 10, respectively), suggesting similar rates of crossovers from SF29 to SF30 or from SF30 to SF29. Interestingly, one local lesion (lesion 98) accumulated a significantly larger number of variant SF29 (13 clones) than of variant SF30 (1 clone).

The results for pair SF29 × SF30 demonstrate that homologous recombination can occur even if one parental RNA3 variant significantly outcompetes the other variant. A similar recombination frequency was obtained for the SF29 × SF30 inoculation (90%) as for the SF23 × SF25 (88%) inoculation.

Seven clones representing the R3 and R4 recombinants were sequenced with primers AB10 and AB4. Five clones had the wt intercistronic regions, while two had silent mutations, i.e., a T to C substitution at position 1009 or an extra A at position 1116, reflecting either the imprecise crossovers or postcrossover mutations. Control RT-PCR amplifications of separate SF29 or SF30 infections, similar to those described above for SF23 or SF25, have confirmed that mutations were not due to the *Taq*1 polymerase errors and were not caused by marker mutations per se (data not shown).

Control coinfections: SF23 × SF29 and SF23 × SF30. To further map the recombinationally active sequences, we have tested the reciprocal pairs of RNA3 recombinants: SF23 × SF29 and SF23 × SF30 (Fig. 1). As shown in Table 1, for the pair SF23 × SF29, all 50 local lesions tested contained only variant SF23, indicating that SF23 outcompetes SF29, which makes the appearance of recombinants difficult. However, for the pair SF23 × SF30, 61 lesions accumulated variant SF23 while 6 contained potential recombinants. Oddly, none of the 67 local lesions analyzed contained the mutant SF30. This result indicates that, similar to SF29, SF30 can be overcome by SF23 (Table 1).

The progeny BMV RNA from six local lesions of the SF23 × SF30 pair were cloned and analyzed (Table 2). In lesion 39, only the parental variants SF23 or SF30 were found, whereas lesions 3, 12, 18, 29, and 50 also accumulated the projected recombinants R2 and R7 (described in Fig. 2). In addition, lesion 50 accumulated the projected recombinant R1. It is important to note that to generate R2 or R7, the crossovers must occur between internal marker mutations. This further supports the potential role of the internal RNA3 region in homologous recombination (see Discussion). To generate R1, the crossovers must occur within the downstream region of RNA3 (encompassing the coat protein open reading frame and a short portion of the 3′ untranslated region).

TABLE 3. Analysis of the cloned cDNA products from the control in vitro RT-PCR reactions using single or mixed BMV RNA3 templates[a]

RNA template(s)	Total no. of clones analyzed	Restriction profile[b]					
		Parental	SF23	SF25	SF29	SF30	Recombinants
Single							
SF23	3	3					
SF25	14	14					
SF29	3	3					
SF30	10	10					
Mixed							
SF23 × SF25	11		4	7			0
SF23 × SF29	14		12		2		0
SF23 × SF30	11		4			7	0
SF29 × SF30	8				3	5	0

[a] The table summarizes the results of the control in vitro recombination experiments during the RT-PCR amplifications using the indicated transcribed BMV RNA3 templates (see Materials and Methods for experimental details).

[b] The numbers represent the number of the individual types of recombinants (indicated) that have been identified as having the particular type of restriction profile.

Control RT-PCR amplifications. The in vitro-transcribed RNA3 variants (SF23, SF25, SF29, and SF30) were amplified separately by RT-PCR, using the same conditions and the same primers described above. As shown in Table 3, all the generated fragments had the expected parental restriction profiles and none revealed abolished *Bam*HI or *Bcl*I sites, indicating that under the experimental conditions used, the RT-PCR amplifications did not generate sequence alterations affecting the restriction sites.

Sequencing analyses of 20 clones per RT-PCR amplification of the in vitro-transcribed SF RNA3 variants have revealed only one (A-to-G) sequence change within the intercistronic region (data not shown). This confirmed that the sequence alterations observed in the intercistronic region of the progeny RNA (see above) were generated during infection, either via RNA recombination or by replicase errors, rather than in the RT-PCR amplifications (see Discussion).

Four mixtures of the in vitro-transcribed RNA3 preparations (SF23 × SF25, SF23 × SF29, SF29 × SF30, and SF23 × SF30) were amplified by RT-PCR. The cDNA products were cloned and analyzed. As shown in Table 3, none of the 43 analyzed clones displayed any of the recombinant profiles, confirming that the RT-PCR in vitro amplifications did not generate the recombinants observed in vivo.

DISCUSSION

In this paper we report the generation of several distinct BMV RNA3 variants by homologous recombination. We found that pairs of the RNA3 molecules, which coreplicate and

coaccumulate in local lesions, can recombine with each other and thus provide a useful homologous recombination assay system. The recombinants can accumulate in the RNA3 populations with no or low selection pressure (mutants SF23 × SF25). In fact, the recombinants accumulated even when a competing pair (SF29 × SF30) of RNA3 was used: the recombinants were observed in 90% of doubly infected lesions, compared to 88% for the less competing SF23 × SF25 combination. This demonstrates that recombination between two BMV RNA3 variants can be readily identified in local lesions.

The recombinant, double-marker, full-length RNA3 cDNA clones were not the RT-PCR artifacts but were formed in planta during the life cycle of the virus. This suggests that neither the RT nor the *Taq* DNA polymerase can support the template exchanges in vitro at comparable levels. However, the in vivo formation of RNA recombinants may be promoted by a much larger number of RNA replication cycles during infection compared to that during the RT-PCR amplifications. Therefore, to compare the template-switching abilities among these three polymerases, the frequency of the BMV RNA crossovers must be studied in vitro.

The difference in the recombination frequency between pairs SF23 × SF25 and SF29 × SF30 is relatively small and cannot be attributed to the distance between marker mutations (1.73 and 0.46 kb, respectively). This result, as well as the fact that infection with the highly competitive pair SF29 × SF30 generated recombinants, suggests the existence of a homologous recombination hot spot within the internal region between the SF29 and SF30 markers. The nucleotide alterations in the progeny RNA3 recombinants, which have occurred close to the genomic region, may reflect the template-switching positions in the imprecise homologous crossovers. However, these alterations may have also arisen due to copying errors by BMV replicase. Further experiments are required to differentiate between these possibilities.

Interestingly, a related observation was made during the in vitro synthesis of full-length transcripts from the cDNA of RNA3. The occurrence of a shorter transcript (nearly 850 nt) was demonstrated (data not shown) using either the T7 or SP6 RNA polymerase or the enzyme mix of the MEGAscript T7 Kit (Ambion). This was not observed when the cDNA of RNA1 and RNA2 were used as templates. The shorter RNA3 transcripts most probably correspond to a fall-off product at the intercistronic region and suggest the existence of a pausing signal, which may operate not only with the T7 or SP6 RNA polymerases but also with the BMV RdRp replicase.

The following mechanisms can be responsible for promoting homologous crossovers within the intercistronic region. A poly(A) [poly(U)] track may facilitate the RdRp slippage, so that the enzyme could change templates during either plus- or minus-strand synthesis. The polymerase slippage has been described for several nucleic acid polymerases (4, 7, 10, 11, 15, 32). Another factor enhancing recombination might be the predicted secondary-structure elements that may act as pausing signals for the RdRp, thus facilitating the template switching. Relatively stable hairpins are predicted within the intercistronic regions of the RNA3 component of BMV, broad bean mottle virus, and cowpea chlorotic mottle virus (36). Secondary-structure-dependent evolution was described for cymbidium ringspot virus defective interfering RNAs (16). Also, a large portion of the intercistronic region constitutes the subgenomic RNA promoter, which could act as an internal reattachment site for the RdRp complex (38). Finally, plus strands of RNA3 may function as intergenic replication enhancers, which probably recruit the RNA3 templates into the replication complex (39). Along these lines, Gennadiy et al. have suggested that in barley yellow dwarf virus, the subgenomic promoter of the barley yellow dwarf virus RNA1 could act as a recombination hot spot in the family *Luteoviridae* (14).

Previously, we have demonstrated that homologous recombination crossovers among different BMV RNA segments could occur at the AU-rich/GC-rich sequences (27, 28, 30). It would be interesting to show whether similar trends could exist during crossovers between the same type (i.e., RNA3) of RNA molecules. Mapping of the homologous recombination hot spots on all three BMV RNA segments is required to find common characteristics of the recombinationally active sequences and the mechanism(s) of these processes.

Most of the supporting data for the role of recombination in RNA virus evolution came from phylogenetic analysis of different virus genes (37). Our results provide new perspectives on the role of homologous RNA recombination in RNA virus evolution. The frequent occurrence of RNA3-RNA3 crosses suggests that the progeny viral RNAs represent a mosaic composed of fragments of different parental RNA templates. According to this model, viral RdRp could jump among the homologous RNAs during replication before completing the replication cycle. Genetically, then, RNA viruses contain multiple copies of the genome that participate in recombination. Such a polyploidal nature not only can provide an efficient pathway to the variability of the viral RNA genome but also can randomize RNA sequences, thereby smoothing out the effects of the errors of RNA replication. Besides genetic recombination, other phenomena that require at least two parental genomes per cell include gene complementation and phenotypic mixing.

Overall, we have shown that the crossovers can occur frequently between homologous RNAs during BMV RNA replication in vivo. Homologous recombination can play an important role in generation the diversity in the RNA virus genome and can provide variants for natural selection that warrants rapid virus evolution. Homologous crossovers are not easily detectable in nature, since they require marker mutations. Our approach of using the coreplicating RNA variants should allow researchers to study such factors of viral RNA recombination as host dependence, virus dependence, and RNA sequence dependence under natural conditions.

ACKNOWLEDGMENTS

We thank N. Rauffer-Bruyere for helpful discussions and P. Brown for editorial comments.

This work was supported by grants from the National Institute for Allergy and Infectious Diseases (3RO1 AI26769), National Science Foundation (MCB-96SF30794), and the U.S. Department of Agriculture (96-39210-3842) and by the Plant Molecular Biology Center at Northern Illinois University.

REFERENCES

1. **Agol, V. I.** 1997. Recombination and other genomic rearrangements in picornaviruses. Semin. Virol. **8:**77–84.
2. **Ahlquist, P.** 1992. Bromovirus RNA replication and transcription. Curr. Opin. Genet. Dev. **2:**71–76.
3. **Allison, R., C. Thompson, and P. Ahlquist.** 1990. Regeneration of a functional RNA virus genome by recombination between deletion mutants and requirement for cowpea chlorotic mottle virus 3a and coat genes for systemic infection. Proc. Natl. Acad. Sci. USA **87:**1820–1824.
4. **Aranda, A., J. E. Perezortin, C. Moore, and M. L. Delolmo.** 1998. Transcription termination downstream of the *Saccharomyces cerevisiae* FBP1 (changed from FPB1) poly(A) site does not depend on efficient 3′ end processing. RNA **4:**303–318.
5. **Banner, L. R., and M. M. C. Lai.** 1991. Random nature of coronavirus RNA recombination in the absence of selection pressure. Virology **185:**441–445.
6. **Banner, L. R., J. G. Keck, and M. M. C. Lai.** 1990. A clustering of RNA recombination sites adjacent to a hypervariable region of the peplomer gene of murine coronavirus. Virology **175:**548–555.

7. **Birse, C. E., B. A. Lee, K. Hansen, and N. J. Proudfoot.** 1997. Transcriptional termination signals for RNA polymerase II in fission yeast. EMBO J. **16:** 3633–3643.
8. **Bujarski, J. J., and P. D. Nagy.** 1996. Different mechanisms of homologous and nonhomologous recombination in brome mosaic virus: role of RNA sequences and replicase proteins. Semin. Virol. **7:**363–372.
9. **Bujarski, J. J., P. D. Nagy, and S. Flasinski.** 1994. Molecular studies of genetic RNA-RNA recombination in brome mosaic virus. Ads. Virus Res. **43:**275–302.
10. **Debrauwere, H., C. G. Gendrel, S. Lechat, and M. Dutreix.** 1997. Differences and similarities between various tandem repeat sequences: minisatellites and microsatellites. Biochimie **79:**577–586.
11. **Deng, L., and S. Shuman.** 1997. Elongation properties of vaccinia virus RNA polymerase: pausing, slippage, 3′ end addition, and termination site choice. Biochemistry **36:**15892–15899.
12. **Figlerowicz, M., and J. J. Bujarski.** 1998. RNA recombination in brome virus, a model plus strand RNA virus. Acta Biochim. Pol. **45:**847–868.
13. **Flasinski, S., A. Dzianott, S. Pratt, and J. J. Bujarski.** 1995. Mutational analysis of the coat protein gene of brome mosaic virus: effects on replication and movement in Barley and *Chenopodium hybridum*. Mol. Plant-Microbe Interact. **8:**23–31.
14. **Gennadiy, K., B. R. Mohan, and W. A. Miller.** 1999. Primary and secondary structural elements required for synthesis of barley yellow dwarf virus subgenomic RNA1. J. Virol. **73:**2876–2885.
15. **Hausmann, S., J. P. Jacques, and D. Kolakofsky.** 1996. Paramyxovirus RNA editing and the requirement for hexamer genome length. RNA **2:**1033–1045.
16. **Havelda, Z., T. Dalmay, and J. Burgyan.** 1997. Secondary structure-dependent evolution of cymbidium ringspot virus defective interfering RNA. J. Gen. Virol. **78:**1227–1234.
17. **Janda, M., R. French, and P. Ahlquist.** 1987. High efficiency T7 polymerase synthesis of infectious RNA from cloned brome mosaic virus cDNA and effects of 5′ extensions of transcript infectivity. Virology **158:**259–262.
18. **Jarvis, T. C., and K. Kirkegaard.** 1992. Poliovirus RNA recombination: mechanistic studies in the absence of selection. EMBO J. **11:**3135–3145.
19. **King, A. M. Q.** 1988. Genetic recombination in positive strand RNA viruses, p. 149–185. *In* E. Domingo, J. J. Holland, and P. Ahlquist (ed.), RNA genetics, vol. 2. CRC Press, Inc., Boca Raton, Fla.
20. **Kirkegaard, K., and D. Baltimore.** 1986. The mechanism of RNA recombination in poliovirus. Cell **47:**433–443.
21. **Koetzner, C. A., M. M. Parker, C. S. Ricard, L. S. Sturman, and P. S. Masters.** 1992. Repair and mutagenesis of the genome of a deletion mutant of the coronavirus mouse hepatitis virus by targeted RNA recombination. J. Virol. **66:**1841–1848.
22. **Lai, M. M. C.** 1992. RNA recombination in animal and plant viruses. Microbiol. Rev. **56:**61–79.
23. **Makino, S., J. O. Fleming, J. G. Keck, S. A. Stohlman, and M. M. C. Lai.** 1987. RNA recombination of coronaviruses: localization of neutralizing epitopes and neuropathogenic determinants on the carboxyl terminus of peplomers. Proc. Natl. Acad. Sci. USA **84:**6567–6571.
24. **Nagy, P. D., and J. J. Bujarski.** 1992. Genetic recombination in brome mosaic virus: effect of sequence and replication of RNA on accumulation of recombinants. J. Virol. **66:**6824–6828.
25. **Nagy, P. D., and J. J. Bujarski.** 1993. Targeting the site of RNA-RNA recombination in brome mosaic virus with antisense sequences. Proc. Natl. Acad. Sci. USA **90:**6390–6394.
26. **Nagy, P. D., and J. J. Bujarski.** 1995. Efficient system of homologous RNA recombination in brome mosaic virus: sequence and structure requirements and accuracy of crossovers. J. Virol. **69:**131–140.
27. **Nagy, P. D., and J. J. Bujarski.** 1997. Engineering of homologous recombination hotspots with AU-rich sequences in brome mosaic virus: AU-rich sequences decrease the accuracy of crossovers. J. Virol. **71:**3799–3810.
28. **Nagy, P. D., and J. J. Bujarski.** 1998. Silencing homologous RNA recombination hot spots with GC-rich sequences in brome mosaic virus. J. Virol. **72:**1122–1130.
29. **Nagy, P. D., and A. E. Simon.** 1997. New insights into the mechanisms of RNA recombination. Virology **235:**1–9.
30. **Nagy, P. D., C. Ogiela, and J. J. Bujarski.** 1999. Mapping sequences active in homologous recombination in brome mosaic virus: prediction of recombination hot-spots. Virology **254:**92–104.
31. **Palasingam, K., and P. N. Shaklee.** 1992. Reversion of Qβ RNA phage mutants by homologous RNA recombination. J. Virol. **66:**2435–2442.
32. **Pathak, V. K., and W.-S. Hu.** 1997. "Might as well jump!" Template switching by retroviral reverse transcriptase, defective genome formation, and recombination. Semin. Virol. **8:**141–150.
33. **Rao, A. L. N., B. P. Sullivan, and T. C. Hall.** 1990. Use of *Chenopodium hybridum* facilitates isolation of brome mosaic virus recombinants. J. Gen. Virol. **71:**1403–1407.
34. **Raju, R., S. V. Subramanian, and M. Hajjou.** 1995. Genesis of Sindbis virus by in vivo recombination of nonreplicative RNA precursors. J. Virol. **69:** 7391–7401.
35. **Romanova, L. I., V. M. Blinov, E. A. Tolskaya, E. G. Viktorova, M. S. Kolesnikowa, E. A. Guseva, and V. I. Agol.** 1986. The primary structure of crossover regions of intertypic poliovirus recombinants: a model of recombination between RNA genomes. Virology **155:**202–213.
36. **Romero, J., A. M. Dzianott, and J. J. Bujarski.** 1992. The nucleotide sequence and genome organization of the RNA2 and RNA3 segments in broad bean mottle virus. Virology **187:**671–81.
37. **Roossinck, M. J.** 1997. Mechanisms of plant virus evolution. Annu. Rev. Phytopathol. **35:**191–209.
38. **Siegel, R. W., S. Adkins, and C. C. Kao.** 1997. Sequence-specific recognition of a subgenomic RNA promoter by a viral RNA polymerase. Proc. Natl. Acad. Sci. USA **94:**11238–11243.
39. **Sullivan, M. L., and P. Ahlquist.** 1999. A brome mosaic virus intergenic RNA3 replication signal functions with viral replication protein 1a to dramatically stabilize RNA in vivo. J. Virol. **74:**2622–2632.
40. **Van der Most, R. G., L. Heijnen, W. J. M. Spaan, and R. J. deGroot.** 1992. Homologous RNA recombination allows efficient introduction of site-specific mutations into the genome of coronavirus MHV-A59 via synthetic co-replicating RNAs. Nucleic Acids Res. **20:**3375–3381.
41. **White, K. A., and T. J. Morris.** 1995. RNA determinants of junction site selection in RNA virus defective interfering RNAs. RNA **1:**1029–1040.
42. **Zhang, X., and M. M. C. Lai.** 1994. Unusual heterogeneity of leader-mRNA fusion in a murine coronavirus: implications for the mechanism of RNA transcription and recombination. J. Virol. **68:**6626–6633.